

## FRAGMENTATION OF COLLAPSAR DISKS AND THE PRODUCTION OF GRAVITATIONAL WAVES

ANTHONY L. PIRO AND ERIC PFAHL

Kavli Institute for Theoretical Physics, Kohn Hall, University of California, Santa Barbara, CA 93106;  
piro@kitp.ucsb.edu, pfahl@kitp.ucsb.edu

Accepted for publication in *The Astrophysical Journal*

### ABSTRACT

We argue that gravitational instability in the outer parts of collapsar disks may lead to fragmentation near the radius where helium photodisintegrates, because of the strong cooling provided by this process. This physics sets clear physical scales for the fragmentation conditions and the properties of gravitationally bound clumps. Collapse of a fragment proceeds until the neutrons become degenerate; a neutron star of mass  $\approx 0.1-1 M_{\odot}$  may result. We find that tidal disruption of a fragment and accretion by the central black hole are too rapid to account for the durations of observed X-ray flares from long gamma-ray bursts. Prior to disruption, migration of the fragment is driven by gravitational radiation and disk viscosity, which act together to produce a unique gravitational-wave signature. Advanced LIGO may be able to detect such sources within  $\approx 100$  Mpc.

*Subject headings:* accretion disks — black hole physics — gamma rays: bursts — gravitational waves

### 1. INTRODUCTION

Observations associating long gamma-ray bursts (GRBs) with core-collapse supernovae (Hjorth et al. 2003; Stanek et al. 2003) provide strong support for the collapsar scenario (Woosley 1993; Paczyński 1998; Popham et al. 1999; MacFadyen & Woosley 1999). In this picture, the central  $\approx 3 M_{\odot}$  of a massive star collapses directly to a black hole, while infalling material with higher specific angular momentum forms an accretion disk of mass  $\sim 1 M_{\odot}$ . Viscous stresses in the disk drive material toward the hole at rates of  $\gtrsim 0.1 M_{\odot} s^{-1}$ , which powers relativistic outflows responsible for both the GRB and the supernova. Although this model has many favorable generic features, certain aspects of the stellar collapse and disk evolution remain poorly understood or largely unexplored. New observational results demand augmentation of the simplest versions of the collapsar scenario.

Recent *Swift* observations have revealed that X-ray flares occurring  $\approx 10^2-10^4$  s after the initial burst are quite common (e.g., O’Brien et al. 2006). The flares exhibit a wide range of amplitudes and time scales, and some GRBs show multiple eruptions. Explanations for the flares point to delayed activity of the central engine (e.g., King et al. 2005; Burrows et al. 2005; Proga & Zhang 2006; Perna et al. 2006). In particular, Perna et al. (2006) speculate that an extended collapsar disk may be gravitationally unstable and fragment at large radii, where the viscous time scale coincides with the onset times of the flares. This work prompted us to examine in more detail the physics of the fragmentation process under the extreme conditions of collapsar disks. We also take a fresh look at the observable consequences, with special emphasis on gravitational-wave emission.

Central to the issue of fragmentation in a self-gravitating accretion disk is the cooling rate of the material. If the disk is formally unstable, gravitationally bound clumps appear only if the cooling time is shorter than the orbital period about the central object (e.g., Gammie 2001); these points are reviewed in § 2. Radiation leakage is far too slow in collapsar disks to be an effective coolant (e.g., Narayan et al. 2001). However, such disks have sufficiently high temperatures ( $\gtrsim 1$  MeV) and densities ( $\gtrsim 10^8$  g cm<sup>-3</sup>) that nuclear processes play critical

roles in the energy budget. We argue in § 3 that nuclear photodisintegration is the only energy sink fast enough to permit fragmentation. The condition for gravitational instability and the strong temperature sensitivity of the photodisintegration rate allow us to nicely constrain the location, size, and mass of an unstable clump. Our estimates suggest that a fragment will collapse until it is supported by neutron degeneracy pressure, forming a low-mass ( $\approx 0.1-1 M_{\odot}$ ) neutron star.

As described in § 4, a fragment will be driven toward the black hole as disk stresses and gravitational radiation remove orbital angular momentum. Migration ends with the tidal disruption of the fragment. We calculate the time scales for migration and subsequent accretion, and consider whether fragmentation accounts for the X-ray flares in long GRBs. Assuming that only a single fragment orbits the central black hole, we estimate in § 5 the characteristic gravitational-wave strain from this binary using a total migration rate that includes viscous torques.

### 2. GRAVITATIONAL INSTABILITY IN COLLAPSAR DISKS

Here we consider the conditions for gravitational instability and fragmentation of *steady-state* collapsar disks (see also Narayan et al. 2001; Di Matteo et al. 2002), where the mass inflow rate is constant in radius. The steady-state assumption is a gross simplification, especially at large disk radii (MacFadyen & Woosley 1999), where material in the collapsing star with high specific angular momentum may continue to rain in for many viscous times. Since this region of the disk is the staging ground for our study, our results should be viewed as only rough approximations.

Our background model consists of a central black hole of mass  $M_{\text{BH}}$  surrounded by a Keplerian accretion disk with radially varying orbital frequency  $\Omega = (GM_{\text{BH}}/r^3)^{1/2}$ , surface density  $\Sigma$ , isothermal sound speed  $c_s$ , and vertical scale height  $H = c_s/\Omega$ . Mass flows at a rate of  $\dot{M} = 3\pi\nu\Sigma$  (e.g., Pringle 1981), where  $\nu = \alpha c_s H$  is the usual viscosity prescription (Shakura & Sunyaev 1973). We assume that  $H/r = \eta$  is a fixed parameter, which is physically plausible in the thick, advective outer region of a steady collapsar disk (e.g., Popham et al. 1999). Results below are given in term of the scaled variables  $r_{100} \equiv r/(100GM_{\text{BH}}c^{-2})$ ,  $M_3 \equiv M_{\text{BH}}/3M_{\odot}$ ,  $\dot{M}_1 \equiv \dot{M}/1M_{\odot} s^{-1}$ ,  $\alpha_{0.1} \equiv \alpha/0.1$ , and  $\eta_{0.5} \equiv \eta/0.5$ .

Gravitational instability arises when (Toomre 1964; Goldreich & Lynden-Bell 1965)

$$Q \equiv \frac{\Omega c_s}{\pi G \Sigma} < Q_{\text{crit}} \simeq 1. \quad (1)$$

The value of  $Q_{\text{crit}}$  depends on the disk thickness and the equation of state. The disk equations above imply that  $Q \propto \alpha \eta^3 \dot{M}^{-1} r^{-3/2}$  decreases with  $r$ , and thus instability holds for

$$r_{100} \gtrsim 4 \alpha_{0.1}^{2/3} \eta_{0.5}^2 \dot{M}_1^{-2/3}. \quad (2)$$

When  $Q < Q_{\text{crit}}$ , the linearly unstable mode with the fastest growth rate ( $\approx \Omega/Q$ ) has a wavelength of  $\approx QH$  and mass of (e.g., § 6.3 of Binney & Tremaine 1987)

$$(QH)^2 \Sigma \approx 0.02 Q^2 \alpha_{0.1}^{-1} M_3 \dot{M}_1 r_{100}^{3/2} M_\odot. \quad (3)$$

We identify  $(QH)^2 \Sigma$  with the mass of a bound clump if cooling is rapid enough to permit collapse (see § 3).

Numerical simulations of thin disks with idealized equations of state and cooling prescriptions show that gravitational instability leads to fragmentation when the cooling time scale satisfies  $\Omega t_{\text{cool}} < \xi$ , where  $\Omega \approx 70 M_3^{-1} r_{100}^{-3/2} \text{ s}^{-1}$ , and  $\xi \approx 1-10$  (e.g., Gammie 2001; Mejía et al. 2005; Rice et al. 2005). When cooling is slow, gravitational instability produces spiral waves that dissipate as thermal energy, driving the disk back toward stability. It is unclear if we can reliably use previous simulations to draw conclusions about collapsar disks, but we take these results as a plausible starting point.

### 3. COOLING MECHANISMS

Using the disk equations in § 2, we evaluate the discriminant  $\Omega t_{\text{cool}} = \Omega \Sigma c_s^2 / qH$  for various possible cooling mechanisms, where  $q$  is the relevant cooling rate in units of  $\text{erg s}^{-1} \text{ cm}^{-3}$ . Cooling via radiative diffusion can be ignored outright, since huge optical depths lead to photon diffusion times of many years (Narayan et al. 2001).

The most important neutrino cooling processes are  $e^\pm$  pair annihilation to neutrinos and the Urca process. We adopt the corresponding cooling rates in Popham et al. (1999). These rates are strong functions of disk temperature, which for an ideal gas is  $T_{10} \equiv T/10^{10} \text{ K} \approx 3.6 \mu \eta_{0.5}^2 M_3 r_{100}^{-1} \text{ K}$ , where  $\mu$  is the mean molecular weight. Here we assume for calculational purposes that material at  $r_{100} > 1$  is pure helium ( $\mu = 4/3$ ) and has the ideal-gas equation of state. At the radius where  $Q = Q_{\text{crit}}$  (see eq. [2]), cooling from pair annihilation gives

$$(\Omega t_{\text{cool}})_{\text{pair}} \approx 800 \alpha_{0.1}^{7/3} \eta_{0.5}^{-9} M_3^{-3} \dot{M}_1^{-7/3}, \quad (4)$$

A similar calculation for Urca cooling yields

$$(\Omega t_{\text{cool}})_{\text{Urca}} \approx 30 \alpha_{0.1}^{7/3} \eta_{0.5}^{-3} M_3^{-1} \dot{M}_1^{-7/3} X_{\text{nuc}}^{-1}, \quad (5)$$

where  $X_{\text{nuc}}$ , the mass fraction of free nucleons, is very sensitive to  $T$  (e.g., Popham et al. 1999). Both  $(\Omega t_{\text{cool}})_{\text{pair}}$  and  $(\Omega t_{\text{cool}})_{\text{Urca}}$  seem too large to allow fragmentation when  $\alpha_{0.1} \approx 1$  (a natural choice for self-gravitating disks; Gammie 2001; Rice et al. 2005) and  $X_{\text{nuc}} \approx 1$ . While we can not rule out pair annihilation as a relevant coolant (for instance, when  $\alpha_{0.1} \approx 0.1$ ), Urca cooling is important only where nuclear photodisintegration is nearly complete. As we now demonstrate, photodisintegration itself will absorb sufficient energy quickly enough to allow fragmentation.

For photodisintegration of  ${}^4\text{He}$  we set

$$(\Omega t_{\text{cool}})_{\text{photo}} = \frac{\Omega c_s^2}{E \lambda} \approx 20 \eta_{0.5}^2 M_3^{-1} r_{100}^{-5/2} \lambda^{-1}, \quad (6)$$

where  $E = 7.07 \text{ MeV}/m_p$  is the  ${}^4\text{He}$  binding energy per nucleon and  $\lambda$  is the reaction rate in  $\text{s}^{-1}$ . Experiments show that the  ${}^4\text{He}(\gamma, n){}^3\text{He}$  and  ${}^4\text{He}(\gamma, p)\text{T}$  cross sections rise abruptly at photon energies of  $\approx 20 \text{ MeV}$  to a plateau value of  $\sigma \approx 1 \text{ mb}$  ( $10^{-27} \text{ cm}^2$ ; Feldman et al. 1990). Subsequent photodisintegration steps have larger cross sections and smaller threshold energies (Skopid et al. 1981; Birenbaum et al. 1985), contributing little to the overall rate. At temperatures  $kT \lesssim 20 \text{ MeV}$  ( $T_{10} \lesssim 23.2$ ), we approximate the  ${}^4\text{He}$  photodisintegration cross section as a step function and integrate over the Wien tail of the Planck spectrum to estimate

$$\lambda \approx 10^{17} T_{10} \exp\left(-\frac{23.2}{T_{10}}\right) \text{ s}^{-1}, \quad (7)$$

which is a good fit to detailed calculations provided to us by H. Schatz (2006, private communication). Because of the exponential factor,  $\lambda$  varies from  $\approx 1$  to  $\approx 10^9$  as  $T_{10}$  is increased from 0.6 to 1.2. Thus, photodisintegration turns on sharply at  $r_{100} \approx 6 \eta_{0.5}^2$ , interior to which  $(\Omega t_{\text{cool}})_{\text{photo}}$  plummets to  $\ll 1$ . Rapid photodisintegration may initiate at slightly larger radii if a gravitationally unstable clump has some compressional heating as it begins to collapse.

It seems that photodisintegration is a very effective coolant, permitting fragmentation over a small range of radii near the location where  $Q = Q_{\text{crit}}$  in the unperturbed disk. By substituting the radius at which  $Q \simeq 1$  (see eq. [2]) into eq. (3), we estimate the mass of a bound fragment:

$$M_f \approx 0.2 \eta_{0.5}^3 M_3 M_\odot. \quad (8)$$

Multiple fragments may form in the same region (e.g., Rice et al. 2005), although it is unclear how their individual masses are distributed. We assume in §§ 4 and 5 that small fragments merge into a single body of mass  $\approx 0.1-1 M_\odot$ .

The breakdown of  ${}^4\text{He}$  into free neutrons and protons has two added benefits. First, efficient Urca cooling becomes possible, promoting the continued collapse of the fragment. Second, as photodisintegration proceeds and  $X_{\text{nuc}}$  approaches unity, the adiabatic pressure-density exponent  $\Gamma_1 \equiv (\partial \log P / \partial \log \rho)_{\text{ad}}$  may dip below  $4/3$ , in which case the gravitationally bound fragment is unstable and collapses dynamically. This second point is illustrated by Imshennik & Nadezhin (1966), who compute the thermodynamic properties of a plasma composed of  ${}^{56}\text{Fe}$ ,  ${}^4\text{He}$ , neutrons, protons, electrons, and positrons. We have repeated these calculations<sup>1</sup> without  ${}^{56}\text{Fe}$ . Figure 1 shows the results in the temperature-density plane, where we see that the trajectories of our disk models pass through the region with  $\Gamma_1 < 4/3$ . However, the overlap of  $Q < Q_{\text{crit}}$  (thick, solid curves) and  $\Gamma_1 < 4/3$  occurs only for sufficiently high  $\dot{M}$  (e.g.,  $\gtrsim 1 M_\odot \text{ s}^{-1}$ ).

Collapse of the fragment halts once the density is high enough for neutron degeneracy to provide pressure support. At this point we might expect the fragment's radius to be

<sup>1</sup> The assumption of thermodynamic equilibrium is not strictly valid unless the material is opaque to neutrinos (Beloborodov 2003), but the approach of Imshennik & Nadezhin (1966) is still useful as an illustrative tool.

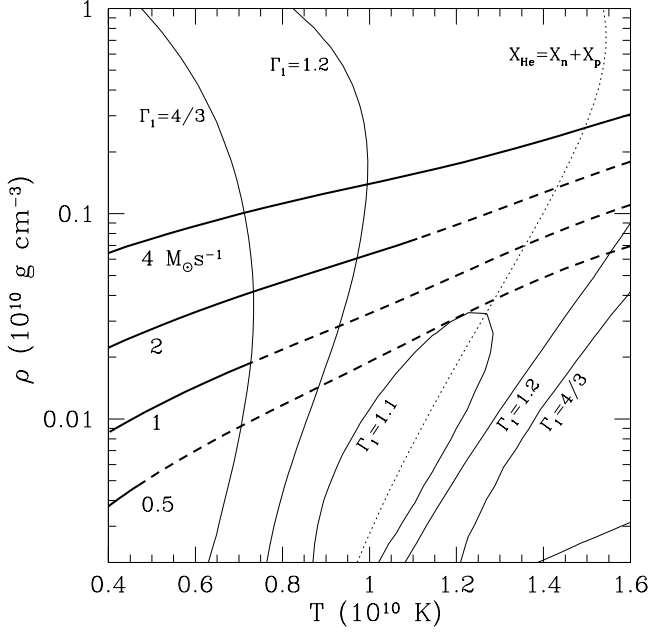


FIG. 1.— Properties of a plasma composed of  ${}^4\text{He}$ , protons, neutrons, electrons, and positrons as a function of density and temperature. The thin solid lines are contours of constant  $\Gamma_1$ , and the thin dotted line marks the half photodisintegration contour ( $X_{\text{He}} = X_n + X_p$ ). Thick lines represent disk models with  $\alpha = 0.1$ ,  $\eta = 0.5$ , and the accretion rates shown. Dashed and solid portions of these curves indicate whether the disk is gravitationally stable or unstable ( $Q < Q_{\text{crit}}$ ), respectively.

$R_f \approx 10(M_f/M_\odot)^{-1/3}$  km. However, there are numerous uncertainties regarding the formation and ultimate structure of this newly formed low-mass neutron star, including the hydrodynamics of the collapse, the equation of state, the effects of the neutrino pressure and finite temperature, and the fate of the fragment if  $M_f \lesssim 0.1 M_\odot$ , the minimum mass of a stable neutron star (e.g., Colpi et al. 1989). An accurate, quantitative assessment of these uncertainties is not possible at present.

#### 4. MIGRATION AND TIDAL DISRUPTION

A net torque on the orbit of the fragment arises from dissipation within the disk and the loss of orbital angular momentum in the form of gravitational waves. When the fragment is massive enough to open a gap in the disk, it migrates inward on the viscous time scale  $r/\dot{r} \approx r^2/\nu$  (i.e., type II migration; Lin & Papaloizou 1986), or

$$t_\nu \approx (\alpha\eta^2\Omega)^{-1} \approx 1\alpha_{0.1}^{-1}\eta_{0.5}^{-2}M_3r_{100}^{3/2}\text{ s}. \quad (9)$$

Gap formation is expected when  $M_f/M_{\text{BH}} \gtrsim \alpha^{1/2}\eta^2 \approx 0.08\alpha_{0.1}^{1/2}\eta_{0.5}^2$  (e.g., Takeuchi et al. 1996), a result derived in relation to planet formation. For simplicity, we adopt  $t_\nu$  as the migration time from disk torques, even if the gap condition is not strictly satisfied. Loss of orbital angular momentum in gravitational waves causes inspiral on a time (Peters 1964)

$$t_{\text{gw}} = \frac{5}{64\Omega} \left( \frac{G\mathcal{M}}{c^3} \Omega \right)^{-5/3} \approx 700\mathcal{M}_1^{-5/3}M_3^{8/3}r_{100}^4\text{ s}, \quad (10)$$

where  $\mathcal{M} \equiv \mathcal{M}_1M_\odot \approx M_f^{3/5}M_{\text{BH}}^{2/5}$  is the chirp mass. The two migration times are equal when the orbital frequency is

$$\Omega_{\text{eq}} \approx \frac{c^3}{G\mathcal{M}} \left( \frac{5\alpha\eta^2}{64} \right)^{3/5} \simeq 4.8\alpha_{0.1}^{3/5}\eta_{0.5}^{6/5}\mathcal{M}_1^{-1}\text{ kHz}. \quad (11)$$

For  $\Omega > \Omega_{\text{eq}}$ , gravitational radiation yields the dominant torque. Both  $\Omega t_\nu \gg 1$  and  $\Omega t_{\text{gw}} \gg 1$  when  $r \gg GM_{\text{BH}}/c^2$ , so that an initially circular orbit remains nearly circular during migration. Also note that efficient neutrino cooling at  $r_{100} \lesssim 1$  allows the disk to thin substantially ( $\eta \approx 0.1\text{--}0.3$ ; Popham et al. 1999), increasing  $t_\nu$  and decreasing  $\Omega_{\text{eq}}$ . This is important in § 5, where we estimate the gravitational-wave signal.

Tidal disruption of the fragment begins when it fills its Roche lobe of radius  $\approx 0.5r(M_f/M_{\text{BH}})^{1/3}$ . If the fragment has the radius of a neutron-degenerate object (see § 3) disruption occurs at frequency

$$\Omega_{\text{dis}} \approx 3.5(M_f/M_\odot)\text{ kHz}. \quad (12)$$

Whether the fragment is disrupted dynamically or undergoes stable mass transfer driven by gravitational radiation (e.g., Bildsten & Cutler 1992), most of the fragment's mass is stripped in  $< 1$  s.

Given the short time for disruption, it seems unlikely that fragmentation of the sort discussed here and in Perna et al. (2006) can account for the late-time X-ray flares in long GRBs, which have rise and decay times similar to their onset times of  $\gtrsim 10^2$  s. Moreover, if a fragment forms at  $r_{100} \approx 1\text{--}4$  and viscous stresses set the migration time to  $\approx 10\text{--}100$  s, accretion of the fragment might blend with the prompt emission. The migration timescale may be increased if the fragment is especially massive in comparison to the disk (Clarke & Syer 1996), but probably by a factor of  $< 10$ . Better understanding of the interaction between the fragment and the disk will require detailed hydrodynamical simulations. Gravitational instability at large disk radii may power the GRB flares, but, if so, probably through enhanced angular momentum transport rather than fragmentation.

#### 5. DETECTION OF GRAVITATIONAL WAVES

LIGO and similar detectors, such as VIRGO, GEO600, and TAMA300, are sensitive to gravitational waves with frequencies of  $\sim 10\text{--}10^3$  Hz. For the full range of GRB models, gravitational waves in the LIGO band would be generated within the central engine, either the compact binary progenitor of a short burst or in a collapsar disk. Measurement of the gravitational-wave signal from a GRB would be a unique probe of the physics at the heart of the explosion (see Kochanek & Piran 1993; Finn et al. 1999; van Putten 2001; Kobayashi & Mészáros 2003). Previous work on gravitational radiation from collapsar disks have addressed general nonaxisymmetric instabilities in compact accretion tori (van Putten 2001) or bar-mode instabilities (Kobayashi & Mészáros 2003). Unlike these earlier scenarios, the simplest form of our fragmentation model constrains the mass quadrupole moment and its evolution, features we now exploit to obtain the gravitational-wave signal.

As in the previous section, we imagine a binary composed of a single fragment in a circular orbit around the black hole. The measured gravitational-wave strain is  $h(t) = h_0(t)\cos\phi(t)$ , where  $f \equiv 100f_{100}\text{ Hz} = \Omega/\pi$  is the slowly varying wave frequency, and  $\phi = 2\pi \int dtf$  is the accumulated phase. For a source at distance  $D = 100D_{100}\text{ Mpc}$ , the strain amplitude is

$$h_0 = \Theta \frac{G\mathcal{M}}{c^2D} \left( \frac{\pi G\mathcal{M}}{c^3} f \right)^{2/3} \simeq 6.4 \times 10^{-24} \Theta \mathcal{M}_1^{5/3} f_{100}^{2/3} D_{100}^{-1}, \quad (13)$$

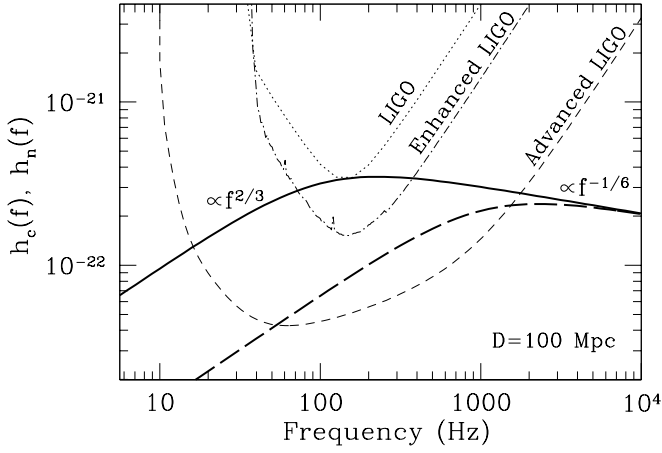


FIG. 2.— Characteristic gravitational-wave strain  $h_c(f)$  from the inspiraling black-hole/fragment binary for  $f_{\text{eq}} = 100$  Hz (thick solid line) and 1 kHz (thick dashed line). Both curves assume  $\mathcal{M} = 1 M_{\odot}$ ,  $D = 100$  Mpc, and  $\Theta = 2.5$ . The thin lines show the broadband strain noise for current LIGO (dotted), enhanced LIGO<sup>2</sup> (dot-dashed), and advanced LIGO (dashed).

where  $\Theta = 0-4$  is a factor incorporating the orientation of the source and the antenna pattern of the detector (e.g., Finn & Chernoff 1993). For completely random source orientations and positions on the sky, the root-mean-square of  $\Theta$  is  $\sqrt{\langle \Theta^2 \rangle} = 1.6$ . Long GRBs seem to be narrowly beamed, probably in a direction normal to the accretion disk. Therefore, we expect an associated black-hole/fragment binary to have a low inclination, which gives  $\sqrt{\langle \Theta^2 \rangle} \simeq 2.5$ , or  $\simeq 60\%$  larger than the random case (see also Kochanek & Piran 1993). In what follows, we let  $\Theta = 2.5$ .

When the waveform is known, the matched filter approach can be used to search for the signal. The signal-to-noise for a slow binary inspiral is then (e.g., Flanagan & Hughes 1998)

$$\left(\frac{S}{N}\right)^2 = \int d(\ln f) n_{\text{cyc}}(f) \frac{h_0^2(f)}{h_n^2(f)}, \quad (14)$$

where  $n_{\text{cyc}} \equiv f^2/\dot{f}$  is the number of cycles per unit  $\ln f$ , and  $h_n$  is the strain noise in a bandwidth  $\approx f$  centered on  $f$ . We see that  $\sqrt{n_{\text{cyc}}}$  is the signal gain and  $\sqrt{n_{\text{cyc}}} h_0 \equiv h_c$  is the associated characteristic strain.

If  $|\dot{r}/r| = \dot{r}_v^{-1} + \dot{r}_{\text{gw}}^{-1}$  is the total inward migration rate from § 4, then  $n_{\text{cyc}} = 2fr/3\dot{r}$ . Some minor algebra yields

$$n_{\text{cyc}}(f) = \frac{2}{3} f t_{\text{gw}} \left[ 1 + \left( \frac{f_{\text{eq}}}{f} \right)^{5/3} \right]^{-1}, \quad (15)$$

<sup>2</sup> For further information see "Enhanced LIGO", LIGO internal document T060156-01-I, R. Adhikari, P. Fritschel, and S. Waldman available at <http://www.ligo.caltech.edu/docs/T/T060156-01.pdf>

where  $f_{\text{eq}} = \Omega_{\text{eq}}/\pi$  (see eq. [11]) tunes the importance of viscous torques. When  $f \ll f_{\text{eq}}$  viscous migration dominates and  $h_c \propto f^{2/3}$ , while gravitational-wave driven inspiral ( $f \gg f_{\text{eq}}$ ) gives  $h_c \propto f^{-1/6}$ . Figure 2 shows  $h_c(f)$  for  $f_{\text{eq}} = 100$  Hz and 1 kHz. The lower value of  $f_{\text{eq}}$  essentially assumes that the disk is fairly thin ( $\eta \approx 0.1$ ), as expected when neutrino cooling is efficient. Since  $h_c$  is peaked near  $f_{\text{eq}}$ , albeit rather broadly, we can use the approximation  $S/N \approx h_c(f_{\text{eq}})/h_n(f_{\text{eq}})$ . Inspection of Figure 2 indicates that, for  $D_{100} \sim 1$ ,  $S/N \approx 5-10$  when  $f_{\text{eq}} = 100$  Hz, while  $S/N \lesssim 1$  when  $f_{\text{eq}} = 1$  kHz. Detection with advanced LIGO seems quite possible for nearby GRBs. The combined effects of viscous torques and gravitational-wave emission on the orbital evolution create a distinct strain signal, where an estimate of  $f_{\text{eq}}$  would provide unique insight into the physics of collapsar disks.

Estimates of the local rate of detectable long GRBs span  $\approx 0.1-1 \text{ Gpc}^{-3} \text{ yr}^{-1}$  (e.g., Guetta et al. 2005), based largely on a small sample with moderate to high redshifts. This implies a rate of  $\lesssim 4 \times 10^{-3} D_{100}^3 \text{ yr}^{-1}$  within a distance  $D$ . However, two GRBs in the past 8 years within 150 Mpc (980425 and 060218; e.g., Galama et al. 1998; Ferrero et al. 2006) suggest tentatively that the local rate is more uncertain and could be as large  $\approx 0.1 D_{100}^3 \text{ yr}^{-1}$ , which is consistent with  $10^{-4}$  of the local rate of core-collapse supernovae (Cappellaro et al. 1999). Beaming implies there may be  $\approx 100$  unseen GRBs for every detectable event, giving a total local GRB rate of  $\lesssim 10 D_{100}^3 \text{ yr}^{-1}$ . If a misdirected GRB is detected by multiple gravitational-wave antennae, it may be possible to locate the source to within a few degrees and provide a target region to search for an "orphaned" electromagnetic afterglow.

We are grateful to Lars Bildsten for critical comments, Scott Hughes for suggestions on a previous draft, and Hendrik Schatz for sharing photodisintegration rates. We thank Rana Adhikari and David Shoemaker for providing LIGO noise strain estimates. We also thank Andrei Beloborodov, Wen-Xin Chen, and William Lee for answering questions about collapsar disks. This work was supported by NSF grant PHY 99-07949 and by the Joint Institute for Nuclear Astrophysics through NSF grant PHY 02-16783.

## REFERENCES

- Beloborodov, A. M. 2003, ApJ, 588, 931  
Bildsten, L., & Cutler, C. 1992, ApJ, 400, 175  
Binney, J., & Tremaine, S. 1987, Galactic Dynamics (Princeton Univ Press: Princeton)  
Birenbaum, Y., Kahane, S., & Moreh, R. 1985, Phys. Rev. C, 32, 1825  
Burrows, D. N., et al. 2005, Science, 309, 1833  
Cappellaro, E., Evans, R., & Turatto, M. 1999, A&A, 351, 459  
Clarke, C. J., & Syer, D. 1996, MNRAS, 278, L23  
Colpi, M., Shapiro, S. L., & Teukolsky, S. A. 1989, ApJ, 339, 318  
Di Matteo, T., Perna, R., & Narayan, R. 2002, ApJ, 579, 706  
Feldman, G., Balbes, M. J., Kramer, L. H., Williams, J. Z., Weller, H. R., & Tilly, D. R. 1990, Phys. Rev. C, 42, 1167  
Ferrero, P., et al. 2006, A&A, 457, 857  
Finn, L. S., & Chernoff, D. F. 1993, Phys. Rev. D, 47, 2198  
Finn, L. S., Mohanty, S. D., & Romano, J. D. 1999, Phys. Rev. D, 60, 121101  
Flanagan, É. É., & Hughes, S. A. 1998, Phys. Rev. D, 57, 4535  
Galama, T. J., et al. 1998, Nature, 395, 670  
Gammie, C. F. 2001, ApJ, 553, 174  
Goldreich, P. & Lynden-Bell, D. 1965, MNRAS, 130, 125  
Guetta, D., Piran, T., & Waxman, E. 2005, ApJ, 619, 412

- Hjorth, J et al., 2003, *Nature*, 423, 847  
Imshennik, V. S. & Nadezhin, D. K. 1966, *Sov. Astron.* 9, 896  
King, A. et al. 2005, *ApJ*, 630, L113  
Kobayashi, S., & Mészáros, P. 2003, *ApJ*, 589, 861  
Kochanek, C. S., & Piran, T. 1993, *ApJ*, 417, L17  
Lin, D. N. C., & Papaloizou, J. C. B. 1986, *ApJ*, 309, 846  
MacFadyen A. I. & Woosley S. E. 1999, *ApJ*, 524, 262  
Mejía, A. C., Durisen, R. H., Pickett, M. K., & Cai, K. 2005, *ApJ*, 619, 1098  
Narayan, R., Piran, T., & Kumar, P. 2001, *ApJ*, 557, 949  
O'Brien, P. T., et al. 2006, *ApJ*, 647, 1213  
Paczynski, B. 1998, *ApJ*, 494, L45  
Perna, R., Armitage, P. J., & Zhang, B. 2006, *ApJ*, 636, L29  
Peters, P. C. 1964, *Physical Review*, 136, 1224  
Popham R., Woosley S.E., & Fryer C. 1999, *ApJ*, 518, 356  
Pringle, J. E. 1981, *ARA&A*, 19, 137  
Proga, D., & Zhang, B. 2006, *MNRAS*, 370, L61  
Rice, W. K. M., Lodato, G., & Armitage, P. J. 2005, *MNRAS*, 364, L56  
Shakura, N. I., & Sunyaev, R. A. 1973, *A&A*, 24, 337  
Skopid, D. M., Beck, D. H., Asai, J., & Murphy, J. J. 1981, *Phys. Rev. C* 24, 1791  
Stanek, K et al., 2003, *ApJ*, 591, L17  
Takeuchi, T., Miyama, S. M., & Lin, D. N. C. 1996, *ApJ*, 460, 832  
Toomre, A. 1964, *ApJ*, 139, 1217  
van Putten, M. H. P. M. 2001, *ApJ*, 562, L51  
Woosley, S.E. 1993, *ApJ*, 405, 273